

NASA/TP-2000-209864



Range and Energy Straggling in Ion Beam Transport

*John W. Wilson and Hsiang Tai
Langley Research Center, Hampton, Virginia*

March 2000

The NASA STI Program Office . . . in Profile

Since its founding, NASA has been dedicated to the advancement of aeronautics and space science. The NASA Scientific and Technical Information (STI) Program Office plays a key part in helping NASA maintain this important role.

The NASA STI Program Office is operated by Langley Research Center, the lead center for NASA's scientific and technical information. The NASA STI Program Office provides access to the NASA STI Database, the largest collection of aeronautical and space science STI in the world. The Program Office is also NASA's institutional mechanism for disseminating the results of its research and development activities. These results are published by NASA in the NASA STI Report Series, which includes the following report types:

- **TECHNICAL PUBLICATION.** Reports of completed research or a major significant phase of research that present the results of NASA programs and include extensive data or theoretical analysis. Includes compilations of significant scientific and technical data and information deemed to be of continuing reference value. NASA counterpart of peer-reviewed formal professional papers, but having less stringent limitations on manuscript length and extent of graphic presentations.
- **TECHNICAL MEMORANDUM.** Scientific and technical findings that are preliminary or of specialized interest, e.g., quick release reports, working papers, and bibliographies that contain minimal annotation. Does not contain extensive analysis.
- **CONTRACTOR REPORT.** Scientific and technical findings by NASA-sponsored contractors and grantees.

- **CONFERENCE PUBLICATION.** Collected papers from scientific and technical conferences, symposia, seminars, or other meetings sponsored or co-sponsored by NASA.
- **SPECIAL PUBLICATION.** Scientific, technical, or historical information from NASA programs, projects, and missions, often concerned with subjects having substantial public interest.
- **TECHNICAL TRANSLATION.** English-language translations of foreign scientific and technical material pertinent to NASA's mission.

Specialized services that complement the STI Program Office's diverse offerings include creating custom thesauri, building customized databases, organizing and publishing research results . . . even providing videos.

For more information about the NASA STI Program Office, see the following:

- Access the NASA STI Program Home Page at <http://www.sti.nasa.gov>
- Email your question via the Internet to help@sti.nasa.gov
- Fax your question to the NASA STI Help Desk at (301) 621-0134
- Telephone the NASA STI Help Desk at (301) 621-0390
- Write to:
NASA STI Help Desk
NASA Center for AeroSpace Information
7121 Standard Drive
Hanover, MD 21076-1320

NASA/TP-2000-209864



Range and Energy Straggling in Ion Beam Transport

*John W. Wilson and Hsiang Tai
Langley Research Center, Hampton, Virginia*

National Aeronautics and
Space Administration

Langley Research Center
Hampton, Virginia 23681-2199

March 2000

Available from:

NASA Center for Aerospace Information (CASI)
7121 Standard Drive
Hanover, MD 21076-1320
(301) 621-0390

National Technical Information Service (NTIS)
5285 Port Royal Road
Springfield, VA 22161-2171
(703) 605-6000

Abstract

A first-order approximation to the range and energy straggling of ion beams is given as a normal distribution for which the standard deviation is estimated from the fluctuations in energy loss events. The standard deviation is calculated by assuming scattering from free electrons with a long range cutoff parameter that depends on the mean excitation energy of the medium. The present formalism is derived by extrapolating Payne's formalism to low energy by systematic energy scaling and to greater depths of penetration by a second-order perturbation. Limited comparisons are made with experimental data.

Introduction

In space radiation transport, the energy loss through atomic collisions is treated as averaged processes over the many events which occur over very small dimensions of most materials and is referred to as the "continuous slowing down approximation" (ref. 1). The small percent fluctuation in energy loss is thought to have little meaning for ions of broad energy spectra and especially in comparison with the many nuclear events for which uncertainties are still relatively large. The exception of course is in the laboratory testing of potential shielding materials with nearly monoenergetic ion beams in which the interpretation of the interaction of the ion beam with shield materials requires a detailed description of the interaction process for comparison with detector responses. In addition to the validation of physical processes, a theoretical model of the role of straggling is essential to understanding the radiobiology of ion beams as required in evaluation of astronaut risks that must be minimized at least to within some regulated level.

Energy and range straggling received considerable attention with the development of accelerated ion beams and the associated advancement of detector technology. The fluctuations of signals in detector responses were often a confusing factor in particle detection, with considerable emphasis given during the late 1950's and throughout the 1960's (refs. 2 and 3). More recently with the development of radiation therapy beams, the issue of range and energy straggling take on added importance because the beam properties near the end of the particle trajectory become an essential part of session planning. Generally such issues are studied experimentally (ref. 3), but a workable theory would greatly enhance the understanding of the radiobiology and improve therapy protocols. With the emergence of new biomedical

accelerators, there is increased activity in the understanding of ion beam characteristics.

Unlike the theory of stopping power, which has well-founded roots in quantum theory (ref. 4), most of the practical methods for energy fluctuations still rely on a simple modification of Rutherford's scattering formula. The assumption is that the energy transfer is like free electron scattering with a low-energy cutoff determined by the atomic/molecular binding properties (refs. 4 and 5). Even then the theory is applicable at best to only 85 to 90 percent of the ion range and only at energies above a few to several MeV/nucleon. In this paper, an attempt is made to find a well-defined extrapolation procedure to overcome these limitations to make them practical in ion beam models. Clearly, extending the theory applicability would be desirable, but this is beyond the scope of the present task. At the minimum, future experiments will allow empirical corrections arriving at a more accurate formalism similar to the analysis of experimental data using a parametric stopping power formalism.

Transport Theory

The specification of the interior environment of a spacecraft and evaluation of the effects on the astronaut is at the heart of the space radiation protection problem. The Langley Research Center has been developing such techniques and an in-depth presentation is given in reference 1 although considerable progress has been made since that publication. The relevant transport equations are the linear Boltzmann equation derived on the basis of conservation principles (ref. 1) for the flux density $\phi_j(x, \Omega, E)$ of type j particles as

$$\begin{aligned} \Omega \cdot \nabla \phi_j(x, \Omega, E) = & \Sigma \int \sigma_{jk}(\Omega, \Omega', E, E') \\ & \times \phi_k(x, \Omega', E') d\Omega' dE' - \sigma_j(E) \phi_j(x, \Omega, E) \end{aligned} \quad (1)$$

where $\sigma_j(E)$ and $\sigma_{jk}(\Omega, \Omega', E, E')$ are the media macroscopic cross sections with $\sigma_{jk}(\Omega, \Omega', E, E')$ representing all those processes by which type k particles moving in direction Ω' with energy E' produce a type j particle in direction Ω with energy E . Note that there may be several reactions which produce a particular product, and the appropriate cross sections for equation (1) are the inclusive ones. The total cross section $\sigma_j(E)$ with the medium for each particle type of energy E may be expanded as

$$\sigma_j(E) = \sigma_{j,at}(E) + \sigma_{j,el}(E) + \sigma_{j,r}(E) \quad (2)$$

where the first term refers to collision with atomic (at) electrons, the second term is for elastic (el) nuclear scattering, and the third term describes nuclear reactions (r). The microscopic cross sections and average energy transfer are ordered as follows:

$$\sigma_{j,at}(E) \sim 10^{-16} \text{ cm}^2 \quad (\Delta E_{at} \sim 10^2 \text{ eV}) \quad (3)$$

$$\sigma_{j,el}(E) \sim 10^{-19} \text{ cm}^2 \quad (\Delta E_{el} \sim 10^6 \text{ eV}) \quad (4)$$

$$\sigma_{j,r}(E) \sim 10^{-24} \text{ cm}^2 \quad (\Delta E_r \sim 10^8 \text{ eV}) \quad (5)$$

This ordering allows flexibility in expanding solutions to the Boltzmann equation as a sequence of physical perturbative approximations. Many atomic collisions ($\approx 10^6$) clearly occur in a centimeter of ordinary matter, whereas $\approx 10^3$ nuclear Coulomb elastic collisions occur per centimeter. In distinction, nuclear reactions are separated by a fraction to many centimeters of condensed matter depending on energy and particle type. Special problems arise in the perturbation approach for neutrons for which $\sigma_{j,at}(E) \approx 0$, and the nuclear elastic process appears as the first-order perturbation.

As noted in the development of equation (1), the cross sections appearing in the Boltzmann equation are the inclusive ones so that the time-independent fields contain no spatial (or time) correlations. However, space- and time-correlated events are functions of the fields themselves and may be evaluated once the fields are known. (See refs. 6 and 7.) Such correlation is important to the biological injury of living tissues. For example, the correlated release of target fragments in biological systems due to ion or neutron collisions have high probabilities of cell injury with low probability of repair resulting in potentially large relative

biological effectiveness (RBE) and quality factor. (See ref. 8.)

The solution of equation (1) involves hundreds of multidimensional integral-differential equations which are coupled together by thousands of cross terms and must be solved self-consistently subject to boundary conditions ultimately related to the external environment and the geometry of the astronaut's body and/or a complex vehicle. To implement a solution one must have the available atomic and nuclear cross-section data, which are a major task in code development.

Transport Coefficients

The transport coefficients relate to the atomic/molecular and nuclear processes by which the particle fields are modified by the presence of a material medium. As such, basic atomic and nuclear theories provide the input to the transport code database. It is through the nuclear processes that the particle fields of different radiation types are transformed from one type to another. The atomic/molecular interactions are the principal means by which the physical insult is delivered to biological systems in producing the chemical precursors to biological change within the cells. The temporal and spatial distributions of such precursors within the cell system govern the rates of diffusive and reactive processes leading to the ultimate biological effects.

Atomic/Molecular Interactions

The first-order physical perturbation to the right-hand side of equation (1) is the atomic/molecular cross sections as noted in equation (3) for which those terms in equation (1) are expanded about the energy moments $S_m(E)$ as

$$S_m(E) = \sum_j \epsilon_j^m \sigma_j(E) \quad (6)$$

where ϵ_j is based on the electronic excitation energy and $\sigma_j(E)$ is the total atomic/molecular cross section for delivering ϵ_j energy to the orbital electrons (including discrete and continuum levels). The first moment ($m = 1$) is the usual stopping power, and the usual continuous slowing down approximation (csda) is achieved by neglecting the higher order energy moments. The second energy moment is related to energy/range straggling and provides corrections to

the ion slowing down spectrum (ref. 1). Equation (6) is misleadingly simple because specification of ϵ_j and $\sigma_j(E)$ requires a complete knowledge of the atomic/molecular wave functions. A many-body local plasma model has been found useful in approximating the atomic and molecular quantities for the positive energy moments (ref. 1). The current stopping power database is derived semiempirically as the Bethe reduction of equation (6) in terms of mean excitation energies and shell corrections (ref. 1). The usual relativistic correction and the density effect correction of Sternheimer are included (ref. 9).

The passing ions are not the primary mediators of biological injury but rather the secondary electrons generated in atomic collisions which transport the energy lost by the passing ion to the biological medium. The distribution of the electrons about the ion path is critical to evaluation of biological injury (refs. 6 and 7), critical to the evaluation of shield attenuation properties (ref. 8), and fundamental to dosimetric evaluation of astronaut exposure risks. Such effects are likewise governed by equation (1). The next physical perturbation term is the Coulomb scattering by the atomic nucleus and is represented by Rutherford scattering modified by screening of the nuclear charge by the orbital electrons using the Thomas-Fermi distribution for the atomic orbitals. The total nuclear Coulomb cross section found by integrating over the scattering directions is related to the radiation length.

Nuclear Interactions

The extent of the nuclear interaction cross-section database required for the transport of cosmic rays spans most nuclear-reaction physics from thermal energies to energies above tens of GeV/nucleon, including a large number of projectile and target material combinations. The types of cross sections required for the transport involve total yields and secondary energy spectra for one-dimensional transport and double differential cross sections in angle and energy for three-dimensional transport. Fortunately, neutron and proton cross sections have been studied at some length in the past. Nuclear-reaction modeling is required, especially for light and heavy ion projectiles, to understand the basic physical processes, and to extrapolate the limited, available experimental data between projectile energies and projectile-target combinations.

A microscopic theory for the description of nuclear fragmentation is being developed through the study of the summation of the nucleus-nucleus, multiple-scattering series for inclusive reactions where a single reaction species is considered. This approach originated in a theory for high-energy alpha particle fragmentation (ref. 10) and has been extended to recast the abrasion-ablation model in microscopic form (ref. 11). The microscopic theory can be shown (ref. 11) to reduce to the optical-model formulation of abrasion (ref. 12) which in turn reduces to the geometric abrasion model (ref. 13). The microscopic theory represents a unified approach where a single formalism generates all production cross sections required for heavy ion transport. Previously the production of heavy fragments, light ions, and nucleons were treated separately, often with disjoint assumptions. A unified approach is useful because the production spectrum of nucleons and light ions from abrasion correlates directly with the formation of prefragment nuclei and their excitation spectra.

The microscopic approach proceeds by formulating the multiple-scattering series for heavy ion reactions in terms of response functions for an arbitrary number of particle knockouts, appropriate for inclusive reaction theory and generalized to the case of heavy ion abrasion dynamics (ref. 11). The reaction dynamics for fragmentation processes are then unified by the development of a single function, the multiple-scattering amplitude, in terms of the momentum vectors of all secondary reaction products. The reaction cross sections for the various secondaries are then found by considering the phase space for an arbitrary final state where there n particles are abraded from the projectile, leaving a projectile prefragment. The decay of the prefragment nuclei into the final fragment opens the kinematical phase space further, and this description will be required for predicting the final mass yields as well as the momentum distribution of ablated nucleons or nuclei.

The description of the development of the scattering amplitude in terms of abrasion response functions has been made by using the eikonal model. The many-body response functions are being developed as convolutions of one-body response functions with the shell model and a correlated Fermi gas model. The corrections to the eikonal theory are then well-known and include large angle scattering corrections and the

many-body effects contained in the full nuclear propagator. Ablation can then be described by well-known statistical and resonance theories for nominal prefragment excitation energies with a new phenomenon possibly occurring for extremely large values in the excitation energy spectrum. Recent test of the model (called QMSFRG) has been very encouraging for future database generation.

If one replaces the quantum mechanical abrasion cross sections by those for nuclei represented as partially transparent uniform spheres and a semiempirical correction to the surface energy to correct the prefragment excitation energy when the prefragment is far from equilibrium, then one obtains the semiempirical fragmentation model (ref. 14). This model is a highly efficient fragmentation database code and can represent available experimental data, even at relatively low energies when Coulomb trajectory corrections are made (ref. 14). It is not as fundamental a code as the microscopic theory because it is limited by the semiempirical correction and by the assumption that nuclei are uniform spheres.

First-Order Solution Methods

The lowest order approximation to the Boltzmann equation is given in terms of the atomic collision processes as (ref. 1)

$$\begin{aligned} \Omega \cdot \nabla \phi_j(x, \Omega, E) &= \sum \sigma_{n,at}(E + \epsilon_n) \\ &\times \phi_j(x, \Omega, E + \epsilon_n) - \sigma_{j,at}(E) \phi_j(x, \Omega, E) \end{aligned} \quad (7)$$

where ϵ_n represents the atomic/molecular excitation energy levels. Equation (7) is equivalent to a one-dimensional transport along the ray directed by Ω . For simplicity of notation, we use a one-dimensional equation as

$$\begin{aligned} \partial_z \phi_j(z, E) &= \sum \sigma_{n,at}(E + \epsilon_n) \\ &\times \phi_j(z, E + \epsilon_n) - \sigma_{j,at}(E) \phi_j(z, E) \end{aligned} \quad (8)$$

where the subscripts at and j are dropped in the rest of this paper. The boundary condition is taken as

$$\phi(0, E) = \delta(E - E_o) \quad (9)$$

where E_o is the initial energy.

The solution can be written with perturbation theory as

$$\phi^{(0)}(z, E) = \exp(-\sigma z) \delta(E - E_o) \quad (10)$$

$$\phi^{(1)}(z, E) = \sigma z \exp(-\sigma z) \sum g_n \delta(E + \epsilon_n - E_o) \quad (11)$$

$$\begin{aligned} \phi^{(2)}(z, E) &= \frac{(\sigma z)^2}{2!} \exp(-\sigma z) \\ &\times \sum g_n g_m \delta(E + \epsilon_n + \epsilon_m - E_o) \end{aligned} \quad (12)$$

and similarly for higher order terms, where $\delta()$ is the Dirac delta function, and $\epsilon_n \ll E_o$ has been assumed so that σ and $g_n = \sigma_n/\sigma$ are evaluated at E_o . The average energy after penetration of a distance z is given by

$$\langle E \rangle = E_o - \langle \epsilon \rangle \sigma z \quad (13)$$

where the average excitation energy is

$$\langle \epsilon \rangle = \sum \epsilon_n g_n \quad (14)$$

and the sum over n contains discrete as well as continuum terms. The standard deviation (s) about the mean energy is similarly found to be

$$s^2 = \langle (E - \langle E \rangle)^2 \rangle = \langle \epsilon^2 \rangle \sigma z \quad (15)$$

with

$$\langle \epsilon^2 \rangle = \sum \epsilon_n^2 g_n \quad (16)$$

Similar results can be derived for the higher moments of the energy distribution, which depend on atomic/molecular quantities through the g_n terms. Considering the nonlinear dependence of the transported spectrum on the atomic cross sections σ_n , it is surprising that the transported spectral parameters depend linearly on g_n . Equations (13) to (16) apply when $E_o \gg \langle \epsilon \rangle \sigma z$ so that the energy variations in the cross sections can be ignored. The expressions are easily generalized to deep penetration as

$$\langle E(z) \rangle = - \int_0^z S[\langle E(y) \rangle] dy \quad (17)$$

and similarly for the standard deviation where the stopping power $S(E)$ is the first moment of the energy transfer given by equation (6). The degrading particle

energy $\langle E(y) \rangle$ is given by the usual range energy relations

$$R(E) = \int_0^E \frac{dE'}{S(E')} \quad (18)$$

It is clear that $R(E)$ is the average stopping path length for the ions. The corresponding spectrum is taken herein as

$$\phi(z, E) = \frac{\exp\{-[E - \langle E(z) \rangle]^2 / [2s(z)^2]\}}{\sqrt{2\pi} s(z)} \quad (19)$$

where the standard deviation $s(z)$ is given by equation (15) for low penetration and its general evaluation is the subject of the present paper. The usual continuous slowing down approximation is found as $s \rightarrow 0$. The evaluation requires knowledge of the appropriate atomic/molecular cross sections σ_n .

Payne's Quasi-Free Electron Approximation

The means of deriving a first-order approximation from the excitation spectrum of atoms or molecules are given. In practice, the appropriate cross sections and excitation energies are not known, and the details of the calculation with approximate wave functions are tedious. Using a simple approximation which is adequate for a first-order theory is customary (refs. 15 and 16). The cross section is represented by a continuum distribution for a heavy charged particle colliding with free electrons for which a long-range cutoff is introduced as follows. The Rutherford cross section for an atom is given by

$$\frac{d\sigma}{d\varepsilon} = \frac{\pi Z_a Z^2 e^4 (A/m)}{E\varepsilon^2} \quad (20)$$

where Z_a is the number of orbital electrons of the target atom/molecule; Z , the projectile effective charge (atomic number at high energies); A , the projectile mass; m , the electron mass; E , the projectile energy; and ε , the energy delivered to the electron in the collision. The range of ε is given as

$$\varepsilon_{\min} = \frac{I^2}{\varepsilon_{\max}} \leq \varepsilon \leq \varepsilon_{\max} = \frac{4m}{A} E \quad (21)$$

where I is the mean excitation energy usually fitted to experimental data. In this approximation, the effects of tight binding of the inner shell electrons are neglected, and binding effects are included only when ε_{\min} is greater than zero. In this approximation, the stopping power is given as

$$S(E) = \frac{2N\pi Z_a Z^2 e^4 (A/m)}{E} \ln \left[\frac{4(m/A)E}{I} \right] \quad (22)$$

where N is the number of atoms/molecules per unit volume. Two clear limitations of equation (22) exist. First the stopping power will decline at low energies as the collision becomes adiabatic and remains positive definite. Second, shell corrections within the $\ln[\]$ term corrects the positive definiteness to energies on the order of 0.5 A MeV, which leaves only the adiabatic region unrepresented. In evaluation of straggling, we follow Payne and approximate as

$$S(E) = S(E_1) \left(\frac{E_1}{E} \right)^a \quad \left(\frac{E_1}{2} < E < \frac{3E_1}{2} \right) \quad (23)$$

where $E_1 = 5AI/m$ and $a = 1 - [\ln(4mE_1/AI)]^{-1}$. Clearly a global formulation will have to overcome these limitations. Payne solved the Boltzmann equation for the second moment $s^2(z)$ by using equations (20) to (23) and obtained

$$s^2(z) = 2 \frac{mE_o^2}{A} \left[(3a+1) \ln \left(\frac{4mE_o}{AI} \right) \right]^{-1} \left\{ \frac{S[\langle E(z) \rangle]}{S(E_o)} \right\}^2 \times \left\{ 1 - \left[\frac{\langle E(z) \rangle}{E_o} \right]^{3a+1} \right\} \quad (24)$$

where E_o is the initial ion energy and $\langle E(z) \rangle$ is the ion mean energy at penetration depth z . The spectrum at depth z is approximated herein as equation (19). Note that most experimental data are expressed as the full width at half maximum (FWHM) that is related to $s(z)$ as $\tau(z) = 2.355s(z)$.

Two known limitations of Payne's formalism are the limitation at low energies expressed in equation (23) and the failure of equation (24) as z approaches 85 percent of the particle mean range.

Because energy straggling is proportional to the ion energy, we show the evaluation of equation (24) as a ratio of $\tau(z)/E_0$ for incident protons of energies of 5, 10, 20, 50, and 100 MeV in liquid oxygen in figure 1. Note that there is little energy dependence in this ratio over this broad energy range and the highest energies nearly collapse into a single curve depending only on the fraction of penetration depth z/R_0 . Evidence of the failure of equation (24) is seen as the ever rapidly broadening of the transmitted energy spectrum past the 80-percent penetration point. To reach a global formalism we must resolve both limitations.

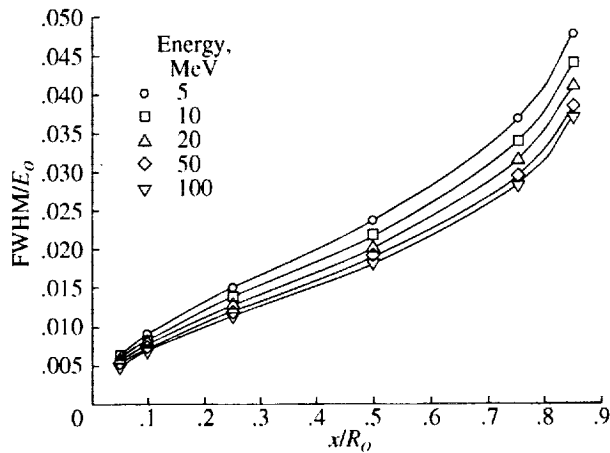


Figure 1. Energy scaled full width at half maximum (FWHM) of energy distribution of monoenergetic proton beam as function of scaled range in liquid oxygen.

Global Formulation of Payne's Method

The spectral dependence given by equation (19) with the variance given by equation (24) has obvious limitations some of which are now resolved. Because equation (19) is the solution for a monoenergetic beam of unit intensity at the boundary, we may use linear superposition to estimate corrections to equation (24). Namely, the fluence of ions at a penetration depth z may be represented as

$$\begin{aligned} \phi(z+z', E) = & \int dE' \frac{\exp \{ -[E' - \langle E(z') \rangle]^2 / 2s'^2(z') \}}{\sqrt{2\pi} s' z} \\ & \times \frac{\exp \{ -[E - \langle E'(z) \rangle]^2 / 2s'^2(z) \}}{\sqrt{2\pi} s'(z)} \end{aligned} \quad (25)$$

where primed quantities are defined at the range z' and are evaluated numerically by using equation (19) with Payne's result, which is equation (24). To the extent that the energy widths are a very small fraction of the energy spectrum over 90 percent of the range, then we may assume that $\langle E'(z) \rangle$ and $s'(z)$ can be evaluated at $E' = \langle E'(z) \rangle$ and the resulting integral in equation (25) may be performed to give

$$\begin{aligned} \phi(z+z', E) &= \frac{\exp \left\{ -[E - \langle E(z) \rangle]^2 / \left\{ 2 \left[s(z')^2 + \tau_{E_0}(z, z') s'(z)^2 \right] \right\} \right\}}{\sqrt{2\pi} \left[s(z')^2 + \tau_{E_0}(z, z') s'(z)^2 \right]} \end{aligned} \quad (26)$$

where

$$\tau_{E_0}(z, z') = \frac{S[\langle E'(z) \rangle]}{S[\langle E(z') \rangle]}$$

The energy spread is shown in figure 2 at different penetration depths in aluminum. We use Payne's original method as equation (24) for depths less than 85 percent of its range. If Payne's approach is carried out all the way to the full range, the width generated is too large as shown in the upper curve for each pair. The widths generated by the two subintervals according to equation (26) are shown as the lower curves. The second limitation of Payne's formalism arises at the lowest energies where the quasi-free approximation is not adequate. We have of course followed

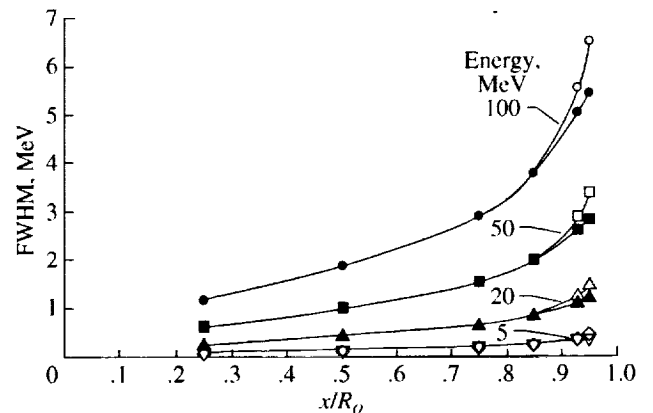


Figure 2. Full width at half maximum (FWHM) of energy distribution of monoenergetic proton beam as function of scaled depth in aluminum. Upper curves near end of range refer to Payne's method; lower curves are modified widths.

Payne's assumptions about the lowest energies in the prior paragraph by the extrapolation to end of the mean range. We extend the lower energies by noting that $s(z)/E_o$ is nearly an energy-independent function of z/R_o by which the result at a given low energy is approximated by extrapolating from a higher energy for the converged functions by energy scaling. For this purpose, the 1 MeV/nucleon energy width $s_1(z)$ is used to scale to lower energies as follows:

$$s(z) = \frac{E s_1 [z R_1 / R(E)]}{1 A} \quad (27)$$

where R_1 is the range of the 1 MeV/nucleon ion.

There is also a conceptual issue to resolve. The energy spectrum at penetration to the mean range ($z = R_o$) is given by

$$\phi(R_o, E) = \frac{\exp[-E^2/2s(R_o)^2]}{\sqrt{2\pi} s(R_o)} \quad (28)$$

where by definition only half the particles penetrate. Those particles of $E > 0$ will continue to penetrate past the mean range. The mean range to stopping is used to estimate the spectrum to larger depths of penetration as follows. For values of $z = R_o + \Delta$, the effects on the spectrum can be estimated by using $\langle E(\Delta) \rangle$ as

$$\phi(\Delta + R_o, E) = \frac{\exp\left\{-[E + \langle E(\Delta) \rangle]^2/2s(R_o)^2\right\}}{\sqrt{2\pi} s(R_o)} \quad (29)$$

which will vanish as Δ becomes large. The resulting total fluence will display an approximate error function dependence with a nearly symmetric decline to zero in the neighborhood of the mean range.

Total Particle Fluence

The total particle fluence as a function of depth is the means by which ion range is defined. The total particle fluence $\Phi(z)$ is given by

$$\Phi(z) = \int \phi(z, E) dE \quad (30)$$

By following the previous formalism, the spectrum at any depth z is written as

$$\phi(z, E) = \frac{\exp[-(E - E_c)^2/2s(z)^2]}{\sqrt{2\pi} s(z)} \quad (31)$$

where $s(z)$ is taken as the value defined by the previous procedure for $z < R_o$ and equal to $s(R_o)$ for larger values of z . The energy E_c is defined as

$$E_c = \begin{cases} \langle E(z) \rangle & (z < R_o) \\ -E(\Delta) & (\Delta = z - R_o > 0) \end{cases} \quad (32)$$

Equations (30) to (32) then result in

$$\Phi(z) = \frac{1 + \text{erf}[E_c/s(z)]}{2} \quad (33)$$

The total fluence is shown for protons in aluminum at energies 5, 50, and 100 MeV in figure 3.

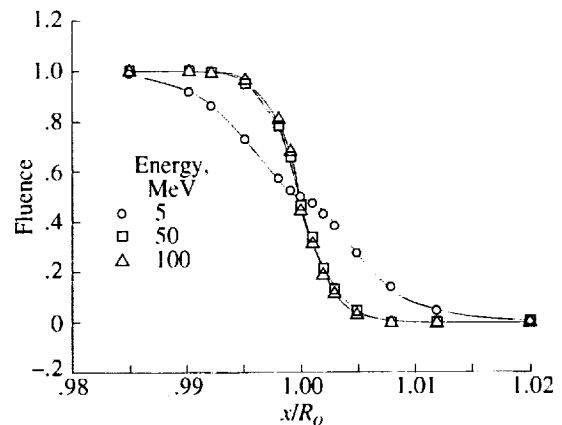


Figure 3. Total particle fluence of proton beam in aluminum near maximum range as function of beam energy.

Comparison With Experiment

Numerical results based on this simple procedure have been obtained and compared with limited experimental data published a long time ago. It is well known that all previous models predicted fairly well in comparison with experimental data when the

penetration is well below 85 percent of the range. However, beyond 85 percent of its range, the models tend to predict a much larger width. This deficiency is corrected by using equation (26) and calculating the Gaussian width at the penetration well beyond 85 percent of its range. Namely, we approximate the width by equation (24) for $z < 0.85R_o$ and extrapolate to larger z with equation (26). The calculated FWHM values and the published experimental values of Tschalär and Maccabee (ref. 3) are given in tables 1 to 3. The experimental values are simply read off the graph from reference 3. With these limited comparisons, tables 1 to 3 seem to establish that our modified model is capable of computing the energy straggling width well within experimental data at the depth covering all the distances of penetration up to the maximum range.

Table 1. Calculated and Experimental Values of FWHM at Different Thickness of Penetration of Proton Beam of 49.10 MeV Energy on Aluminum Target

$$[R_o = 2.8283 \text{ g/cm}^2]$$

Thickness, g/cm ²	FWHM, MeV	
	Calculated	Experimental (ref. 3)
2.605	2.51	2.45
2.675	2.74	3.00
2.713	2.92	3.30
2.745	3.14	3.75
2.760	3.29	4.00
2.785	3.64	4.30
2.802	4.08	4.55
2.820	5.25	4.60

Concluding Remarks

Although the final approach to the straggling problem adopted in the present paper needs further

Table 2. Calculated and Experimental Values of FWHM at Different Thickness of Penetration of Proton Beam of 19.68 MeV Energy on Aluminum Target

$$[R_o = 0.55677 \text{ g/cm}^2]$$

Thickness, g/cm ²	FWHM, MeV	
	Calculated	Experimental (ref. 3)
0.099	0.22	0.26
0.267	0.40	0.45
0.398	0.60	0.62
0.497	0.99	1.10

Table 3. Calculated and Experimental Values of FWHM at Different Thickness of Penetration of Alpha Particle of 79.8 MeV Energy on Aluminum Target

$$[R_o = 0.57023 \text{ g/cm}^2]$$

Thickness, g/cm ²	FWHM, MeV	
	Calculated	Experimental (ref. 3)
0.099	0.43	0.50
0.267	0.80	1.00
0.398	1.17	1.10
0.497	1.84	2.07
0.553	2.73	2.70

development, it does provide a usable formalism which seems to fit the limited experimental data. There is no reason to believe that other ions are not at least as well represented by the present formalism. At least first-order estimates of the ion stopping problem is in hand, and an improved estimate of the near end of range effects on ion transport is now available in a simple computational algorithm.

References

1. Wilson, John W.; Townsend, Lawrence W.; Schimmerling, Walter; Khandelwal, Govind S.; Khan, Ferdous; Nealy, John E.; Cucinotta, Francis A.; Simonsen, Lisa C.; Shinn, Judy L.; and Norbury, John W.: *Transport Methods and Interactions for Space Radiations*. NASA RP-1257, 1991.
2. Maccabee, H. D.; Raju, M. R.; and Tobias, C. A.: Fluctuations of Energy Loss by Heavy Charged Particles in Thin Absorbers. *Phys. Rev.*, vol. 165, no. 2, 1968, pp. 469–474.
3. Tschalär, C.; and Maccabee, H. D.: Energy-Straggling Measurements of Heavy Charged Particles in Thick Absorbers. *Phys. Rev. B*, vol. 1, no. 7, 1970, pp. 2863–2869.
4. Bethe, H. A.: The Range-Energy Relation for Slow Alpha-Particles and Protons in Air. *Rev. Modern Phys.*, vol. 22, no. 2, 1950, pp. 213–219.
5. Manson, Steven T.; Toburen, L. H.; Madison, D. H.; and Stolterfoht, N.: Energy and Angular Distribution of Electrons Ejected From Helium by Fast Protons and Electrons: Theory and Experiment. *Phys. Rev. A*, vol. 12, no. 1, 1975, pp. 60–79.
6. Wilson, John W.; Cucinotta, F. A.; and Shinn, J. L.: Cell Kinetics and Track Structure. *Biological Effects and Physics of Solar and Galactic Cosmic Radiation*, Part A, Charles E. Swenbert, Gerda Horneck, and E. G. Stassinopoulos, eds., Plenum Press, pp. 295–338.
7. Cucinotta, F. A.; Katz, R.; and Wilson, J. W.: Radial Distribution of Electron Spectra From High-Energy Ions. *Radiat. & Environ. Biophys.*, vol. 37, no. 4, 1998, pp. 259–265.
8. Shinn, J. L.; Wilson, J. W.; and Ngo, D. M.: Risk Assessment Methodologies for Target Fragments Produced in High-Energy Nucleon Reactions. *Health Phys.*, vol. 59, no. 1, 1990, pp. 141–143.
9. Shinn, Judy L.; Farhat, Hamidullah; Badavi, Francis F.; and Wilson, John W.: *Polarization Correction for Ionization Loss in a Galactic Cosmic Ray Transport Code (HZETRN)*. NASA TM-4443, 1993.
10. Cucinotta, Francis A.; Townsend, Lawrence W.; and Wilson, John W.: *Description of Alpha-Nucleus Interaction Cross Sections for Cosmic Ray Shielding Studies*. NASA TP-3285, 1993.
11. Cucinotta, Francis A.; and Dubey, Rajendra R.: *Final State Interactions and Inclusive Nuclear Collisions*. NASA TP-3353, 1993.
12. Townsend, L. W.; Wilson, J. W.; Cucinotta, F. A.; and Norbury, J. W.: Comparison of Abrasion Model Differences in Heavy Ion Fragmentation—Optical Versus Geometric Models. *Phys. Rev. C*, vol. 34, no. 4, 1986, pp. 1491–1494.
13. Wilson, John W.; Townsend, Lawrence W.; and Badavi, F. F.: A Semiempirical Nuclear Fragmentation Model. *Nucl. Instrum. & Methods Phys. Res.*, vol. B18, no. 3, 1987, pp. 225–231.
14. Wilson, J. W.; Tripathi, R. K.; Cucinotta, F. A.; Shinn, J. L.; Badavi, F. F.; Chun, S. Y.; Norbury, J. W.; Zeitlin, C. J.; Heilbronn, L.; and Miller, J.: *NUCFR2: An Evaluation of the Semiempirical Nuclear Fragmentation Database*. NASA TP-3533, 1995.
15. Symon, Keith R.: Fluctuations in Energy Lost by High Energy Charged Particles in Passing Through Matter. Ph.D. Thesis, Harvard Univ., Jan. 1948.
16. Payne, M. G.: Energy Straggling by Alpha Particles, Protons, and Other Heavy Charged Particles in Homogeneous Absorbers. *Bull. Am. Phys. Soc.*, vol. 13, 1968, p. 1711.
17. Payne, M. G.: Energy Straggling of Heavy Charged Particles in Thick Absorbers. *Phys. Rev.*, vol. 185, no. 2, 1969, pp. 611–623.

REPORT DOCUMENTATION PAGE			Form Approved OMB No. 0704-0188	
Public reporting burden for this collection of information is estimated to average 1 hour per response, including the time for reviewing instructions, searching existing data sources, gathering and maintaining the data needed, and completing and reviewing the collection of information. Send comments regarding this burden estimate or any other aspect of this collection of information, including suggestions for reducing this burden, to Washington Headquarters Services, Directorate for Information Operations and Reports, 1215 Jefferson Davis Highway, Suite 1204, Arlington, VA 22202-4302, and to the Office of Management and Budget, Paperwork Reduction Project (0704-0188), Washington, DC 20503.				
1. AGENCY USE ONLY (Leave blank)	2. REPORT DATE March 2000	3. REPORT TYPE AND DATES COVERED Technical Publication		
4. TITLE AND SUBTITLE Range and Energy Straggling in Ion Beam Transport			5. FUNDING NUMBERS WU 111-10-95-01	
6. AUTHOR(S) John W. Wilson and Hsiang Tai				
7. PERFORMING ORGANIZATION NAME(S) AND ADDRESS(ES) NASA Langley Research Center Hampton, VA 23681-2199			8. PERFORMING ORGANIZATION REPORT NUMBER L-17866	
9. SPONSORING/MONITORING AGENCY NAME(S) AND ADDRESS(ES) National Aeronautics and Space Administration Washington, DC 20546-0001			10. SPONSORING/MONITORING AGENCY REPORT NUMBER NASA/TP-2000-209864	
11. SUPPLEMENTARY NOTES				
12a. DISTRIBUTION/AVAILABILITY STATEMENT Unclassified-Unlimited Subject Category 93 Distribution: Standard Availability: NASA CASI (301) 621-0390			12b. DISTRIBUTION CODE	
13. ABSTRACT (Maximum 200 words) A first-order approximation to the range and energy straggling of ion beams is given as a normal distribution for which the standard deviation is estimated from the fluctuations in energy loss events. The standard deviation is calculated by assuming scattering from free electrons with a long range cutoff parameter that depends on the mean excitation energy of the medium. The present formalism is derived by extrapolating Payne's formalism to low energy by systematic energy scaling and to greater depths of penetration by a second-order perturbation. Limited comparisons are made with experimental data.				
14. SUBJECT TERMS Ion transport; Energy loss; Straggling			15. NUMBER OF PAGES 14	
			16. PRICE CODE A03	
17. SECURITY CLASSIFICATION OF REPORT Unclassified	18. SECURITY CLASSIFICATION OF THIS PAGE Unclassified	19. SECURITY CLASSIFICATION OF ABSTRACT Unclassified	20. LIMITATION OF ABSTRACT UL	